

Non-universal gauged lepton number for charged lepton masses hierarchy and

$$(g - 2)_{e,\mu}$$

We-Fu Chang^{1,*}

¹*Department of Physics, National Tsing Hua University, Hsinchu, Taiwan 30013, R.O.C.*

(Dated: December 22, 2022)

We construct a novel flavor-dependent gauged lepton number $U(1)_\ell$ model for the hierarchical charged lepton masses and the observed $(g - 2)_{e,\mu}$. Only tau participates in the tree-level Standard Model (SM) Yukawa interaction. At the same time, the masses of electron and muon are light due to radiative generation and(or) the heavy-mediator-suppressed Yukawa coupling to the SM Higgs. Not only can the measured anomalous magnetic dipole moment of the muon, Δa_μ , be explained, but the positive (or negative) Δa_e can also be accommodated in this model.

Without additional discrete symmetries introduced, charged lepton flavor violation is highly suppressed by the $U(1)_\ell$ symmetry. Corresponding to two equally viable $U(1)_\ell$ charge assignments, this model predicts either $A_{FB}^e > A_{FB}^\tau > A_{FB}^\mu$ or $A_{FB}^e < A_{FB}^\tau < A_{FB}^\mu$, which can be tested at the e^+e^- machines before discovering the $U(1)_\ell$ gauge boson. Moreover, the effective muon and electron Yukawa couplings can depart significantly from the SM predictions, and those deviations could be probed at future e^+e^- colliders and High-Luminosity LHC.

I. INTRODUCTION

The observed hierarchy among the charged fermion masses is one of SM's great puzzles. In SM, the charged fermion masses stem from the SM Higgs Yukawa interaction with the predicted relationship $m_f = y_f v_0 / \sqrt{2}$, where y_f is the Yukawa coupling of fermion f and $v_0 \simeq 246\text{GeV}$ is the vacuum expectation value (VEV) of the SM Higgs. Experimentally, the Higgs Yukawa couplings of top[1], bottom[2, 3], tau[4, 5], and muon[6, 7] are consistent, within the errors of \sim a few $\times 10\%$ [8–10], with the SM predictions. The improvement of y_μ determination is promising at High-Luminosity LHC and future e^+e^- colliders[11], and an ultimate precision of $\sim 0.4\%$ is projected at the future FCC[12]. Due to the smallness of y_e , six orders of magnitude smaller than y_t , the current upper limit on electron-Yukawa, $|y_e/y_e^{SM}| < 260$ [13, 14], is relatively poor. However, it is possible to reach a sensitivity of $|y_e/y_e^{SM}| < 1.6$ at FCC-ee in the future[15].

* wfchang@phys.nthu.edu.tw

One interesting speculation about the charged fermion mass hierarchy is that the light charged fermion masses are radiatively generated. Various models of this sort had been proposed a long time ago; see the review[16] and the earlier references therein. For more recent considerations along this line, see [17–29]. For simplicity, we will only consider the lepton sector and construct a model to justify the observed charged lepton mass hierarchy.

On the other hand, combining data from BNL E821 and the result of FNAL gives [30]

$$\Delta a_\mu^{BNL-FNAL} = \Delta a_\mu^{exp} - \Delta a_\mu^{SM} \simeq (25.1 \pm 5.9) \times 10^{-10}. \quad (1)$$

For a comprehensive review of the SM prediction of $(g-2)_\mu$, see [31] and references therein¹. As for the electron, Δa_e can be deduced with the input of fine-structure constant α_{em} . By adopting α_{em} determined by using Cesium atoms[36] or Rubidium atoms[37], Δa_e takes the value

$$\Delta a_e^{Cs} \simeq (-8.7 \pm 3.6) \times 10^{-13} \quad (2)$$

or

$$\Delta a_e^{Rb} \simeq (+4.8 \pm 3.0) \times 10^{-13}, \quad (3)$$

respectively. Note the two values differ by 5.4σ [37], and more investigations are needed to settle the issue. It is still unclear how to resolve this discrepancy in α_{em} determination at this moment, and thus we will consider both, but separately, Δa_e^{Cs} and Δa_e^{Rb} .

The radiative lepton mass generation mechanism closely connects to leptons' anomalous magnetic dipole moments. As long as the Feynman diagrams for radiative mass generation have charged degrees of freedom running in the loop, one can always attach an external photon to one of those charged particles and yield nonzero Δa_l . Reversely, by removing the external photon line from the Feynman diagram(s) for $(g-2)$, a nonzero Δa_l implies a finite radiative mass correction to the lepton. The fact that $m_e, m_\mu \ll m_\tau$ and the observed deviations between $(g-2)_{\mu,e}$ and the SM predictions logically insinuate the possibility that electron and muon masses are radiatively generated.

We point out a novel anomaly-free gauged lepton $U(1)_\ell$ symmetry² to rationalize the observed mass hierarchy $m_e, m_\mu \ll m_\tau$ and accommodate the observed $\Delta a_\mu^{BNL-FNAL}$ and $\Delta a_e^{Cs[Rb]}$. For recent similar attempts, see, for example, [24, 26]. The SM leptons carry different $U(1)_\ell$ charges

¹ The SM prediction of the hadronic vacuum polarisation contribution to the muon $(g-2)$ is still under debate.

The recent lattice calculations[32–35] predict a value consistent with the experimental result of muon $(g-2)$ but are in tension with the leading-order determination obtained by using dispersion relations, see [31].

² See [38–42] for the early discussion on gauged lepton number.

in our model. Within the simple anomaly-free $U(1)_\ell$ charge assignment, one left-handed and one right-handed lepton are $U(1)_\ell$ neutral. We identify the $U(1)_\ell$ neutral lepton as tau, which acquires its mass from the SM Yukawa coupling, while the SM electron and muon Higgs Yukawa interactions are forbidden. In addition to the exotic scalar sector, only one pair of exotic vector fermions, $N_{L,R}$, is introduced in this model. The Dirac mass of vector fermion $N_{L,R}$ plays a vital role in chirality flipping in generating radiative masses and nonzero Δa 's to electron and muon.

A nice feature of our model is the flexibility to separately fit $\Delta a_\mu^{BNL-FNAL}$ with Δa_e^{Cs} or $\Delta a_\mu^{BNL-FNAL}$ plus Δa_e^{Cs} . This adaptability is due to the additional gauge-invariant electron Yukawa coupling to one of the exotic Higgs doublets. Moreover, ad hoc parities or symmetries are usually used to suppress the dangerous charged lepton flavor violating (CLFV) processes³ such as $l_i \rightarrow l_j \gamma$, $l_i \rightarrow l_a l_b l_c$, and μ - e conversion. In our model, the CLFV processes are highly suppressed or forbidden by the automatically emerged accidental symmetries. For the flavor conserving part, this model predicts that the muon and electron effective Yukawa couplings can deviate significantly from their SM predictions, and such abnormal Yukawa couplings can be tested at the future colliders.

In Sec.II, the model is described in detail, and the radiative electron and muon mass generation and $(g-2)_{e,\mu}$ are also analyzed. We demonstrate in Sec.III that CLFV processes are highly suppressed and completely vanishing for tau flavor in this model. In Sec.IV, we discuss the phenomenology of the gauge boson and the effective electron- and muon-Higgs Yukawa couplings. One of the important predictions is that the forward-backward asymmetries of e, μ, τ are different and can be verified experimentally. Before the conclusion, in Sec.V, we briefly address the possible extension of this model to include a dark matter candidate and the neutrino mass generation.

II. MODEL

In this model, the SM leptons carry different $U(1)_l$ charges, see Table I. This model also calls for one pair of vector fermion N , two doublets scalars, $H_{5,3}$, and three singlet scalars, $C_{8,6}, S_3$, see Table II. It is evident that our model is free of anomalies. Note that it is still a viable solution if all $U(1)_l$ charges change sign. However, the sign is physical and can be determined by the interferences between the $U(1)_\ell$ gauge boson and the SM gauge bosons at the future e^+e^- colliders. The vector fermions admit a tree-level Dirac mass term $-M_N(\bar{N}_R N_L + \bar{N}_L N_R)$.

³ For a bottom-up approach to deal with the CLFV constrain, see [43].

	SM lepton	SM Higgs
Symmetry \ Fields	$L_\tau \ L_\mu \ L_e \ \tau_R \ e_R \ \mu_R$	$H = \begin{pmatrix} H^+ \\ H^0 \end{pmatrix}$
$SU(2)_L$	2 1	2
$U(1)_Y$	$-\frac{1}{2}$ -1	$\frac{1}{2}$
$U(1)_\ell$	0 4 -4 0 -7 7	0

TABLE I. The SM fields and their quantum numbers under the SM $SU(2)_L \otimes U(1)_Y$, and the gauged lepton number $U(1)_\ell$.

	New Fermion	New Scalar				
Symmetry \ Fields	$N_{L,R}$	$H_3 = \begin{pmatrix} H_3^0 \\ H_3^- \end{pmatrix}$	$H_5 = \begin{pmatrix} H_5^0 \\ H_5^- \end{pmatrix}$	C_6	C_8	S_3
$SU(2)_L$	1	2	2	1	1	1
$U(1)_Y$	0	$-\frac{1}{2}$	$-\frac{1}{2}$	1	1	0
$U(1)_\ell$	-1	-3	5	6	-8	3

TABLE II. New field content and quantum number assignment under the SM gauge symmetries $SU(2)_L \otimes U(1)_Y$, and the gauged lepton numbers $U(1)_\ell$.

The most general gauge-invariant Yukawa interactions are

$$\begin{aligned}
\mathcal{L} \supset & y_{\mu R} \overline{N}_L \mu_R C_8 + y_{\mu L} \overline{N}_R H_5^\dagger L_\mu + y_{eR} \overline{N}_L e_R C_6 + y_{eL} \overline{N}_R H_3^\dagger L_e \\
& - y_\tau \overline{L}_\tau \tau_R H + y_3 \overline{L}_e e_R \tilde{H}_3 + H.c.
\end{aligned} \tag{4}$$

All the six new Yukawa couplings are complex in general, but only one phase combination is physical after field redefinition. Note that the traditional global lepton number, where all L_i , e_{Ri} , and $N_{L,R}$ carry one unit of the conventional lepton number, is conserved. In addition, this model acquires an accidental discrete symmetry Z_τ under which L_τ and τ_R are odd while all other fields transform trivially. We emphasize that these two accidental symmetries, see Table III, emerge automatically from the anomaly-free $U(1)_\ell$ charge assignment. The $U(1)_\ell$ is assumed to be spontaneously broken by S_3 at an energy scale higher than SM electroweak scale. As S_3 takes its VEV, $\langle S_3 \rangle = v_3/\sqrt{2}$, the $U(1)_\ell$ gauge boson X acquires a mass $M_X = 3g_l v_3$, where g_l is the unknown gauge coupling strength of $U(1)_\ell$.

Here, we focus on the relevant scalar mixing terms

$$\mathcal{L} \supset \mu_{H_3} H^\dagger \tilde{H}_3 S_3^* + \kappa_3 H^\dagger H_3 S_3^* C_6 + \kappa_5 H^\dagger H_5 S_3 C_8 + H.c., \tag{5}$$

Accidental Symmetry \ Fields	L_τ τ_R	$L_\mu, L_e, \mu_R, e_R, N_{L,R}$	$H, H_3, H_5, C_8, C_6, S_3$
global lepton number	1 1	1	0
Z_τ	- -	+	+

TABLE III. The fields and their quantum numbers under the accidental global lepton number and tau parity.

while the complete scalar sector lagrangian and some details can be found in Appendix A. After the SSB of SM electroweak⁴, $\langle H_0 \rangle = v_0/\sqrt{2}$, H_5^+ mixes with C_8^+ , and H_3^+ mixes with C_6^+ . The two charged scalar sectors can be separately diagonalized by two rotations

$$U^{(l)} = \begin{pmatrix} \cos \alpha^{(l)} & \sin \alpha^{(l)} \\ -\sin \alpha^{(l)} & \cos \alpha^{(l)} \end{pmatrix}. \quad (6)$$

The angles are given by

$$\sin 2\alpha^{(\mu)} = \frac{\kappa_5 v_0 v_3}{M_{H^{(e)}}^2 - M_{L^{(e)}}^2}, \quad \sin 2\alpha^{(e)} = \frac{\kappa_3 v_0 v_3}{M_{H^{(\mu)}}^2 - M_{L^{(\mu)}}^2}, \quad (7)$$

where $M_{H^{(e/\mu)}}$ and $M_{L^{(e/\mu)}}$ are the mass eigenvalues of the heavier and lighter charged scalar associated with electron/muon, respectively. Then in terms of the heavy(light) mass eigenstate $\Phi_{H(L)}^{(e)}$,

$$H_5^+ = \cos \alpha^{(\mu)} \Phi_L^{(\mu)} + \sin \alpha^{(\mu)} \Phi_H^{(\mu)}, \quad C_8^+ = -\sin \alpha^{(\mu)} \Phi_L^{(\mu)} + \cos \alpha^{(\mu)} \Phi_H^{(\mu)}. \quad (8)$$

Similarly, for the H_3^+ - C_6^+ pair, we have

$$H_3^+ = \cos \alpha^{(e)} \Phi_L^{(e)} + \sin \alpha^{(e)} \Phi_H^{(e)}, \quad C_6^+ = -\sin \alpha^{(e)} \Phi_L^{(e)} + \cos \alpha^{(e)} \Phi_H^{(e)}. \quad (9)$$

The two 1-loop diagrams shown in Fig.1 give rise to electron and muon radiative masses. The corresponding radiative masses can be easily calculated as

$$m_{loop}^{(e)} = \frac{y_{eR}^* y_{eL}}{32\pi^2} \frac{\kappa_3 v_3 v_0}{M_N} \mathcal{F}_0 \left(\beta_H^{(e)}, \beta_L^{(e)} \right), \quad (10)$$

$$m_{loop}^{(\mu)} = \frac{y_{\mu R}^* y_{\mu L}}{32\pi^2} \frac{\kappa_5 v_3 v_0}{M_N} \mathcal{F}_0 \left(\beta_H^{(\mu)}, \beta_L^{(\mu)} \right), \quad (11)$$

where $\beta_{H/L}^i = \left(\frac{M_{H/L}^i}{M_N} \right)^2$, $i = (e), (\mu)$, and the definition of the loop function can be found in Appendix B. Note that $\mathcal{F}_0(z_1, z_2) = \mathcal{F}_0(z_2, z_1) > 0$ if $z_{1,2} \geq 0$.

⁴ We assume that H_5 and H_3 do not develop VEV.

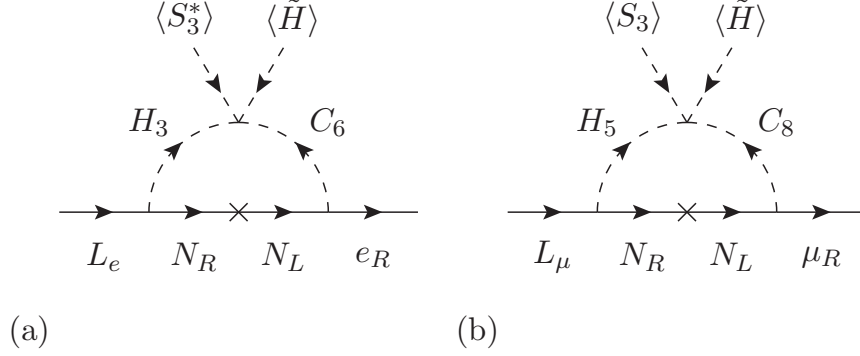


FIG. 1. The Feynman diagrams (in the interaction basis) for $(g-2)_{e,\mu}$, effective Higgs couplings, and the radiative masses for electron and muon. For $g-2$, the photon attaches to the charged scalar in the loop. For the radiative lepton-Higgs Yukawa couplings, one can either replace the Higgs VEV with an external SM Higgs or connect the SM Higgs to the charged scalars.

In addition to the radiatively generated masses, the tree-level Yukawa interaction also yields an effective mass to electron, see Fig.2 where the neutral component H_3^0 is the mediator. Assuming the mixings between H_3^0 and other fields are small, we have

$$m_{tree}^{(e)} = \frac{y_{tree}^{(e)} v_0}{\sqrt{2}}, \quad \text{where } y_{tree}^{(e)} \simeq \frac{y_3 \mu_{H3} v_3}{\sqrt{2} M_3^2}, \quad (12)$$

after integrating out the heavy H_3^0 . And tau acquires its mass $m_\tau = \frac{y_\tau v_0}{\sqrt{2}}$ via the SM Yukawa interaction. Hence, the charged lepton mass matrix,

$$\mathcal{L} \supset -(\overline{e_L}, \overline{\mu_L}, \overline{\tau_L}) \begin{pmatrix} m_{loop}^{(e)} + m_{tree}^{(e)} & 0 & 0 \\ 0 & m_{loop}^{(\mu)} & 0 \\ 0 & 0 & \frac{1}{\sqrt{2}} y_\tau v_0 \end{pmatrix} \begin{pmatrix} e_R \\ \mu_R \\ \tau_R \end{pmatrix} + H.c., \quad (13)$$

is diagonal in this model at the 1-loop level. And it will be clear that the SM CLFV dim-4 operators, $\overline{L}_i e_{Rj} H$ ($j \neq i$), vanish to all orders.

For muon, the phase of $m_{loop}^{(\mu)}$ can be removed by muon chiral field redefinition. Since $\tilde{\mathcal{F}}_0(\beta_H^{(\mu)}, \beta_L^{(\mu)}) > 0$, we can always choose the combination $\kappa_5(y_{\mu R}^* y_{\mu L})$ as a positive real number such that the muon mass is positively defined. Similarly, the phase of the complex y_τ can also be absorbed by redefinition of the tau chiral fields so that y_τ takes a positive real value $y_\tau = \sqrt{2}(m_\tau \text{GeV}/v_0) \simeq 1.02 \times 10^{-2}$.

With one photon attached to the charged scalar in the loop diagrams shown in Fig.1, one can

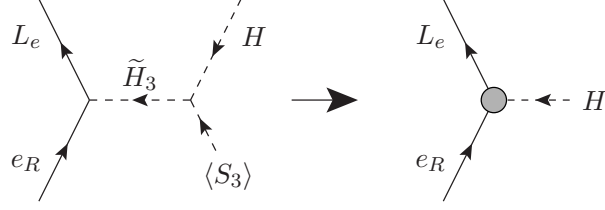


FIG. 2. The Feynman diagram for generating the effective e_R - L_e - H coupling after the SSB of gauged lepton number.

calculate the anomalous magnetic moments of electron and muon. For $m_F \gg m_l$, we have[44]

$$\begin{aligned}\Delta a_e &= \frac{\Re[y_{eR}^* y_{eL}]}{32\pi^2} \frac{m_e}{M_N^2} \frac{\kappa_3 v_3 v_0}{M_N} \tilde{\mathcal{I}}_0 \left(\beta_H^{(e)}, \beta_L^{(e)} \right), \\ \Delta a_\mu &= \frac{\Re[y_{\mu R}^* y_{\mu L}]}{32\pi^2} \frac{m_\mu}{M_N^2} \frac{\kappa_5 v_3 v_0}{M_N} \tilde{\mathcal{I}}_0 \left(\beta_H^{(\mu)}, \beta_L^{(\mu)} \right),\end{aligned}\quad (14)$$

where $m_{e,\mu}$ are the physical lepton masses, and the loop function is given by

$$\tilde{\mathcal{I}}_0 \equiv \frac{\mathcal{J}_0(z_1) - \mathcal{J}_0(z_2)}{z_1 - z_2}, \quad \text{and} \quad \mathcal{J}_0(z) = \frac{1 - z^2 + 2z \ln z}{(z - 1)^3}.\quad (15)$$

Note $\tilde{\mathcal{I}}_0$ is symmetric and positively defined.

For electron and muon, the ratio

$$\frac{\Delta a_l}{m_{loop}^{(l)}} = \frac{m_l}{M_N^2} \frac{\Re[y_{lR}^* y_{lL}]}{y_{lR}^* y_{lL}} \frac{\tilde{\mathcal{I}}_0 \left(\beta_H^{(l)}, \beta_L^{(l)} \right)}{\mathcal{F}_0 \left(\beta_H^{(l)}, \beta_L^{(l)} \right)}\quad (16)$$

is independent of the mixing angle, or equivalently $\kappa_{5,3}$. For muon, $y_{\mu R}^* y_{\mu L}$ can be made a real number by field redefinition or $m_{loop}^{(\mu)} = m_\mu \simeq 0.105\text{GeV}$. Hence, $\Delta a_\mu > 0$ follows and agrees with the sign of the measured $\Delta a_\mu^{BNL-FNAL}$. On the other hand, the tree-level Yukawa contribution mediated by H_3 is reserved for the electron, so either positive or negative $\Delta a_e(m_{loop}^{(e)})$ could be accommodated. Moreover, since m_μ is known, Δa_μ only depends on three physical masses, M_N and $M_{H/L}^{(\mu)}$. In Fig.3 we display the allowed 2-dimensional parameter space of $M_{H/L}^{(\mu)}$, for a given M_N , which gives rise to the observed 1σ range of $\Delta a_\mu^{BNL-FNAL}$. As seen in Fig.3, the typical values for $M_{H/L}^{(\mu)}$ are about a few TeV. We also show the product $y_{\mu R}^* y_{\mu L} s_\alpha^{(\mu)} c_\alpha^{(\mu)}$ vs M_N in Fig.4. For a fixed M_N , we scan the region of $0.2\text{TeV} < M_{L(\mu)} < M_{H(\mu)} < 5\text{TeV}$ to find the viable solution which yields the measured $\Delta a_\mu^{BNL-FNAL}$. The typical value of the mixing product is in the reasonable range of $10^{-2} - 10^{-1}$ for $M_N \in [0.1, 2.0]\text{TeV}$, and the minimum, $\sim 10^{-2}$, happens at around $M_N \sim 1\text{TeV}$. By assuming $|y_{\mu R, \mu L}| < \sqrt{4\pi}$, we obtain a lower bound $|\sin \alpha^{(\mu)}| \gtrsim 10^{-3}$ for $\Delta a_\mu^{BNL-FNAL}$, which is to be accommodated in this model.

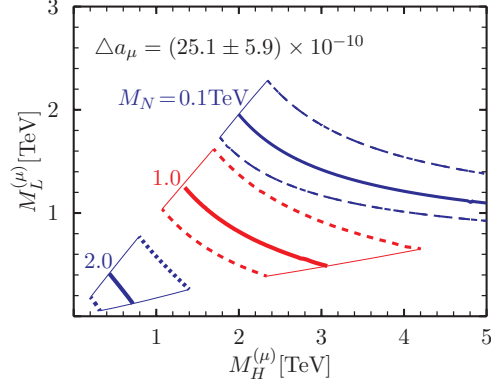


FIG. 3. The 2-dimensional parameter space of $M_{H/L}$ for the muon. The solid(dash) lines represent Δa_μ at the central(1σ boundary) values for $M_N = \{0.1, 1.0, 2.0\}$ TeV.

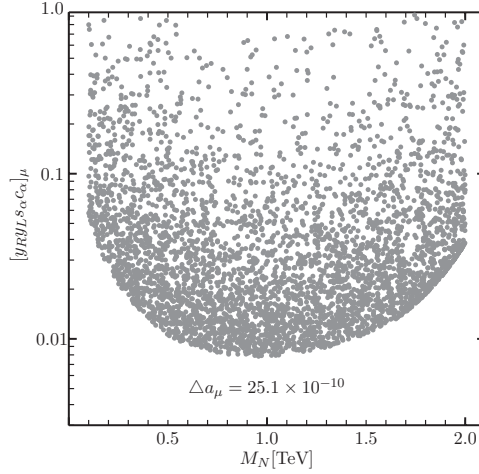


FIG. 4. The mixing product $y_{\mu R}^* y_{\mu L} \sin \alpha^\mu \cos \alpha^\mu$ for muon v.s. M_N for $\Delta a_\mu = 25.1 \times 10^{-10}$.

It is evident that the new physics(NP) contribution to $\Delta a_\tau^{NP} = 0$ at the 1-loop level. The leading contribution to Δa_τ^{NP} is the 2-loop Barr-Zee-like diagrams with charged scalars running in the loop, which gives rise to the effective $\gamma\gamma H_{SM}$ vertex. In this model, the charged scalars are $\phi_{H/L}^{(e,\mu)}$. The ballpark estimation gives

$$\Delta a_\tau^{NP} \sim \frac{\alpha_{em}}{(4\pi^2)^2} \sum_k \frac{\mu_k}{v_0} \frac{m_\tau^2}{M_k^2} \ln \frac{M_h^2}{M_k^2}, \quad (17)$$

where μ_k represents the triple coupling of the charged scalar, of mass M_k , with the SM Higgs, and M_h the SM Higgs mass. Taking $\mu_k \sim v_0$, $M_k \sim \mathcal{O}(\text{TeV})$, this model predicts $|\Delta a_\tau^{NP}| \lesssim \mathcal{O}(10^{-10})$, which is beyond the experimental sensitivities in the near future.

Now we turn our attention to the electron. Since one can only remove one physical CP phase through the field redefinition, it has to be reserved for making the physical mass real positive.

Similar to the calculation of Δa_e , the electric dipole moment of the electron from NP can be derived as

$$d_e^{NP} = -e \frac{\Im[y_{eR}^* y_{eL}]}{64\pi^2} \frac{\kappa_3 v_0 v_3 \tilde{\mathcal{I}}_0}{M_N^3} \left(\beta_H^{(e)}, \beta_L^{(e)} \right). \quad (18)$$

In terms of Δa_e , it can also be expressed as

$$d_e^{NP} = -\frac{e \tan \delta_{CP}^{(e)}}{2m_e} \Delta a_e, \text{ where } \delta_{CP}^{(e)} = \arg(y_{eR}^* y_{eL}). \quad (19)$$

Note that the m_e here is the positive real physical mass. Plugging in the value of $\Delta a_e = -8.7[+4.8] \times 10^{-13}$ and the latest limit on $|d_e| < 1.1 \times 10^{-29} e\text{-cm}$ [45], we obtain a stringent bound that

$$\left| \tan \delta_{CP}^{(e)} \right| < 6.56[3.62] \times 10^{-7}. \quad (20)$$

The phenomenological consideration indicates that the two phases of $m_{tree}^{(e)}$ and $m_{loop}^{(e)}$ are aligned to the level of $\mathcal{O}(10^{-7})$. The smallness of the relative phase, $\delta_{CP}^{(e)}$, cannot be addressed in the current model setup. It suggests that CP symmetry should be assumed, at least for the lepton sector. Therefore, in the rest of the paper, we set $\delta_{CP}^{(e)} = 0$ for simplicity⁵. Then, the overall phase can be removed by electron field redefinition so

$$m_e = y_{tree}^{(e)} \frac{v_0}{\sqrt{2}} + \Delta a_e \frac{M_N^2}{m_e} \tilde{R} \left(\beta_H^{(e)}, \beta_L^{(e)} \right), \text{ where } \tilde{R}(z_1, z_2) \equiv \frac{\mathcal{F}_0(z_1, z_2)}{\tilde{\mathcal{I}}(z_1, z_2)} \quad (21)$$

and $\tilde{R} > 0$. Equivalently, we have

$$y_3 = \frac{6gl}{\sqrt{2} \mu_{H3} M_X} \frac{M_3^2}{m_e} (1 - \bar{R}_e) y_{SM}^{(e)}, \quad \bar{R}_e \equiv \frac{m_{loop}^{(e)}}{m_e} = \Delta a_e \frac{M_N^2}{m_e^2} \tilde{R} \left(\beta_H^{(e)}, \beta_L^{(e)} \right), \quad (22)$$

where $y_{SM}^{(e)} = \sqrt{2} m_e / v_0 = 2.94 \times 10^{-6}$ is the SM electron Yukawa coupling. From Fig.5, we see the typical value of $|\bar{R}_e|$, the ratio of the radiative mass to the physical mass of electron, is about $\sim \mathcal{O}(10)$ for $M_{H,L}^{(e)} \sim \text{TeV}$. If we take $M_N \simeq M_X \simeq 1\text{TeV}$, $M_3 (\sim M_H^{(\mu)}) \simeq 2\text{TeV}$, and $\bar{R}_e \simeq -10$, then

$$y_3^{Cs} \sim 1.497 \times 10^{-2} \times \left(\frac{gl}{0.1e} \right) \times \left(\frac{10\text{GeV}}{\mu_{H3}} \right). \quad (23)$$

On the other hand, if one adopts $\Delta a_e^{Rb} = 4.8 \times 10^{-13}$ and keeps all other parameters fixed, then

$$y_3^{Rb} \sim -0.612 \times 10^{-2} \times \left(\frac{gl}{0.1e} \right) \times \left(\frac{10\text{GeV}}{\mu_{H3}} \right). \quad (24)$$

Compared with $y_{SM}^{(\tau)} = 1.02 \times 10^{-2}$, this model does not need ridiculous fine tuning to yield the observed charged lepton mass hierarchy.

⁵ Note that, in this model, $d_\mu^{NP} = d_\tau^{NP} = 0$ at the 1-loop level even without assuming CP symmetry. On the other hand, if both Δa_e and Δa_μ are positive, one can exchange the identities of electron and muon such that $d_e^{NP} = d_\tau^{NP} = 0$ at the 1-loop level. In that case, d_e^{NP} starts at the 3-loop level and the constraint from d_e^{NP} is much alleviated. Moreover, $d_\mu^{NP} = 2.4 \times 10^{-22} \times \tan \delta_{CP}^{(\mu)} e\text{-cm}$ is safely below the current bound $|d_\mu^{NP}| < 1.8 \times 10^{-19} e\text{-cm}$ [46].

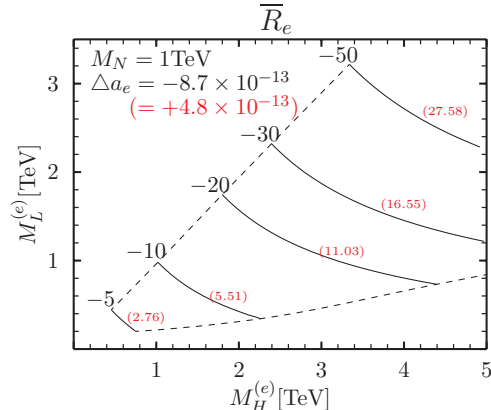


FIG. 5. The contour (solid lines) plot of $\bar{R}_e = m_{loop}^{(e)}/m_e$, while the dashed lines indicate the boundary. We take the values $M_N = 1$ TeV and $\Delta a_e^{Cs} = -8.7 \times 10^{-13}$ as the reference. For different values of Δa_e , the contour values scale linearly in Δa_e . For example, the values in parentheses are for $\Delta a_e^{Rb} = +4.8 \times 10^{-13}$.

III. CHARGED LEPTON FLAVOR VIOLATION

First, note that both the traditional lepton number and the accidental Z_τ parity are intact after the SSB of $U(1)_\ell$. If we follow the fermion line of an incoming tau for any Feynman diagram, it must end up with an outgoing tau. Therefore, there is no tau number violation in this model to all orders, and we only need to consider the CLFV in the electron and muon sectors. Because the SM gauge symmetries are at work in the intermediate energy scale between the SSB of $U(1)_\ell$ and the SSB of the SM electroweak, we address the possible CLFV in the $e - \mu$ sector by considering the SM gauge-invariant operators in terms of SM DOF.

Starting from dim-4, we need to consider only three operators (and their hermitian conjugations),

$$\bar{L}_\mu \gamma^\alpha D_\alpha L_e, \bar{\mu}_R \gamma^\alpha D_\alpha e_R, \bar{L}_\mu e_R H, \quad (25)$$

where D_α is the SM covariant derivative. The first two operators give rise to the CLFV wavefunction corrections, while the last one generates the cross-flavor mass term below the SSB of SM electroweak. The most general Feynman diagrams consist of two external leptons can be pictorially illustrated in Fig.6(a,b), where the gray blobs represent any possible perturbative Feynman diagrams that constitute the vertices. The corresponding $U(1)_\ell$ charges for operators listed in Eq.(25) are $\{-8, -14, -11\}$, respectively. In this model, only H and S_3 are higgsed, thus the injected $U(1)_\ell$ charge can only be $\Delta Q_\ell = 3k$, where k is an integer, corresponding to the number of external S_3 lines above the SSB of $U(1)_\ell$. Therefore, all the dim-4 CLFV operators are forbidden to all orders

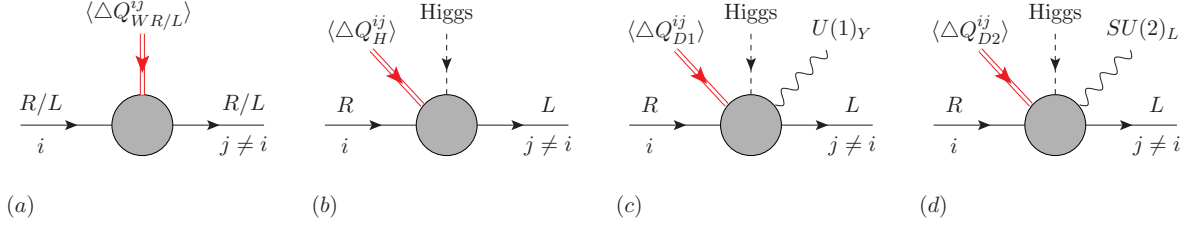


FIG. 6. The dim-4 (a,b) and the dim-6 (c,d) dipole charged lepton flavor changing operators and the required quantum number injection (double line). The gray blobs represent any possible perturbative Feynman diagrams that constitute the vertices. The indices i, j stand for flavor and L/R label the charged lepton chirality.

in this model. And the resulting $h_{SM} \rightarrow \mu e$ from the dim-4 operators also vanishes.

We move on to consider the dim-6 operators. The complete⁶ SM gauge-invariant dimension-6 dipole, Fig.6(c,d), and 4-lepton operators, Fig.7, are

$$\begin{aligned} \tilde{O}_{D1}^{ij} &= (\bar{L}_i \sigma^{\alpha\beta} R_j) H F_{\alpha\beta}, \quad \tilde{O}_{D2}^{ij} = (\bar{L}_i \sigma^{\alpha\beta} \vec{\tau} R_j) H \vec{W}_{\alpha\beta}, \\ \tilde{O}_{LL}^{ijab} &= (\bar{L}_i \gamma^\alpha L_j) (\bar{L}_a \gamma^\alpha L_b), \quad \tilde{O}_{LR}^{ijab} = (\bar{L}_i \gamma^\alpha L_j) (\bar{R}_a \gamma^\alpha R_b), \quad \tilde{O}_{RR}^{ijab} = (\bar{R}_i \gamma^\alpha R_j) (\bar{R}_a \gamma^\alpha R_b), \end{aligned} \quad (26)$$

where $\vec{\tau}$ is the Pauli matrix, $F_{\alpha\beta}$ and $W_{\alpha\beta}$ are the field strengths of $U(1)_Y$ and $SU(2)_L$, respectively. The operators $\tilde{O}_{D1,D2}^{\mu e}$ need +11 $U(1)_\ell$ charge injection and are forbidden to all orders. As a result, the dimension-6 contributions to $\mu \rightarrow e\gamma$ and $Z \rightarrow \mu e$ vanish.

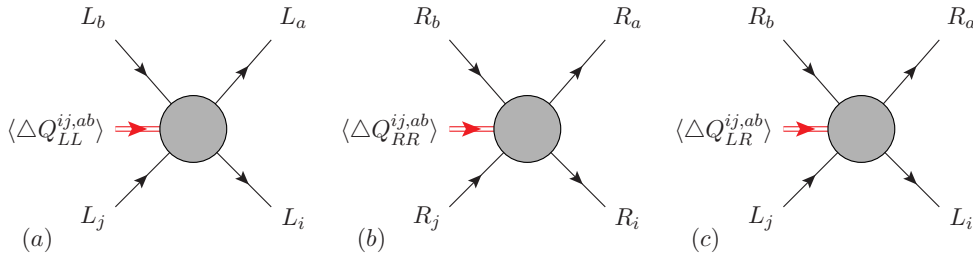


FIG. 7. The general Feynman diagrams for the CLVF 4-lepton operators and the required quantum number injection(double line). The gray blobs represent any possible perturbative Feynman diagrams that constitute the vertices. The indices i, j, a, b stand for flavor, and L/R label the charged lepton chirality.

For the CLFV 4-lepton operators, the required quantum numbers injection (double line in Fig.7) into these blobs are listed in Table IV, where the $(e\mu)(ee)$ column relates to $\mu \rightarrow 3e$, and the $(e\mu)(e\mu)$ column relates to muonium-antimuonium oscillations. Again, only H and S_3 are higgsed

⁶ Note that $(\bar{L}_i \sigma^{\alpha\beta} R_j)(\bar{R}_a \sigma_{\alpha\beta} L_b) = 0$, $(\bar{L}_i \gamma^\alpha \vec{\tau} L_j)(\bar{L}_a \gamma^\alpha \vec{\tau} L_b) = 2\tilde{O}_{LL}^{ibaj} - \tilde{O}_{LL}^{ijab}$, and $-2(\bar{L}_i R_j)(\bar{R}_a L_b) = \tilde{O}_{LR}^{ibaj}$, by using the Fierz transformation and the properties of Pauli matrices.

in this model, and none of the required quantum number injection is possible to all orders. One can easily generalize the analysis to the dim-6 2-lepton-2-quark operators and conclude there is no CLFV 4-fermion operator to all orders in this model setup. The dim-6 operator for μ - e conversion on nuclei is also forbidden.

operator \ (ij)(ab)	$(e\mu)(l_k l_k)$	$(e\mu)(e\mu)$	$(\tau e)(\mu\tau)$
\tilde{O}_{LL}^{ijab}	8	16	-8
\tilde{O}_{RR}^{ijab}	14	28	-14
\tilde{O}_{LR}^{ijab}	8	22	-11
\tilde{O}_{RL}^{ijab}	14	22	-11

TABLE IV. The net $U(1)_\ell$ charge of the CLFV dimension-six 4-lepton operators, where $l_k = e, \mu, \tau$, and i, j, a, b are the flavor indices.

In principle, the RGE evolution could induce CLFV below the electroweak scale from higher dimensional (> 6) operators⁷. Although the general discussion on CLFV operators with dimensions higher than six is beyond the scope of this paper, we expect the RGE running effects to be suppressed and insignificant.

IV. PHENOMENOLOGY

By convention, we will take g_2, g_1, g_l , the gauge coupling strengths, to be positive. Since the SM parts in the covariant derivative

$$D_\mu = \partial_\mu - ig_2 T_3 \vec{\sigma} \cdot \vec{A}_\mu - ig_1 Y B_\mu - ig_l Q_l X_\mu \quad (27)$$

stay the same, we focus on the new gauge $U(1)_l$ interaction part. The leptons interact with the new gauge boson X via

$$\mathcal{L} \supset -ig_l \sum_l \left[\bar{l} \gamma_\mu (G_{lL} \hat{L} + G_{lR} \hat{R}) l \right] X^\mu \quad (28)$$

with $-G_{eL} = G_{\mu L} = 4$, $-G_{eR} = G_{\mu R} = 7$, and $G_{\tau L} = G_{\tau R} = 0$.

If integrating out the heavy X , one obtains an effective contact interaction $\frac{16g_l^2}{M_X^2} (\bar{e}_L \gamma^\alpha e_L) (\bar{\mu}_L \gamma_\alpha \mu_L)$. From the limit[10] $\Lambda^+(ee\mu\mu) > 8.5\text{TeV}$, we get

$$g_l < \sqrt{\frac{\pi}{8}} \left(\frac{M_X}{8.5\text{TeV}} \right) \simeq 0.24e \left(\frac{M_X}{\text{TeV}} \right). \quad (29)$$

⁷ Since only leptons are charged under $U(1)_\ell$, the next order of CLFV relevant operators are dim-10 6-lepton ones. For example, the CLFV vertex with three incoming muons and three outgoing electrons plus one external SM Higgs, which leads to CLFV 2-to-4 scattering $e^- e^- \rightarrow e^+ \mu^- \mu^- \mu^-$, is possible by proper v_3 insertion. Although this general vertex is symmetry allowed, we failed to find the corresponding Feynman diagram(s).

The widths of X decays into fermion and scalar pairs are given by

$$\Gamma_{X \rightarrow l+l^-} = \Theta(1 - 4\beta_l) \frac{g_l^2}{24\pi} M_X [G_{lL}^2 + G_{lR}^2 + 6\beta_f G_{lL} G_{lR}] \sqrt{1 - 4\beta_l}, \quad (30)$$

$$\Gamma_{X \rightarrow SS^*} = \Theta(1 - 4\beta_S) \frac{g_l^2 Q_s^2}{48\pi} M_X (1 - 4\beta_S)^{\frac{3}{2}}, \quad (31)$$

respectively. In the above, Q_s is the $U(1)_\ell$ charge of the scalar S , $\beta_i = (m_i/M_X)^2$, and Θ is the step function. If all the exotic scalars are heavier than $M_X/2$, the decay width of X is dominated by the modes with 2-body e^+e^- , $\mu^+\mu^-$, $\bar{\nu}_e\nu_e$, $\bar{\nu}_\mu\nu_\mu$ final states. One has

$$\frac{\Gamma_X}{M_X} \simeq 27\alpha_{em} \left(\frac{g_l}{e}\right)^2 < 1.17 \times 10^{-2} \left(\frac{M_X}{\text{TeV}}\right)^2, \quad (32)$$

where α_{em} is the fine structure constant, and the upper bound stems from Eq.(29). At the X -pole, the narrow-width gauge boson has a large cross-section

$$\sigma(e^+e^- \rightarrow X^* \rightarrow l^+l^-) = \frac{g_l^4 (G_{eL}^2 + G_{eR}^2)^2}{24\pi M_X^2} \frac{M_X^2}{\Gamma_X^2}, \quad (33)$$

where $l = e, \mu$. For $M_X = 1\text{TeV}$ and $g_l = 0.1e$, this cross-section is about $6.1 \times 10^{10} \text{fb}$. If X boson can be produced at the future high energy e^+e^- collider, the narrow peaks of invariant masses $m_{ee} \sim m_{\mu\mu} \sim M_X$ will be smoking gun evidence of the gauge $U(1)_\ell$. On the other hand, even below the X resonance, the interferences between X and the SM gauge boson cause significant differences in the forward-backward asymmetry of leptons. The formulae of forward-backward asymmetry of leptons have been collected in Appendix C. In Fig.8, we display the A_{FB} of three leptons by assuming that $M_X = 1\text{TeV}$, $g_l = 0.1e$, $Q_i^N = -1$, and X only decays into a lepton pair. Since tauon does not couple to X , it follows the SM prediction. Due to the different $U(1)_l$ charges, A_{FB}^e and A_{FB}^μ differ from the SM prediction significantly. At the Z -pole, $A_{FB}^e/A_{FB}^\tau \sim 1.0001$ and $A_{FB}^\mu/A_{FB}^\tau \sim 0.9999$. However, the current experimental precision cannot tell the differences at Z -pole. The differences grow and reach $\sim \mathcal{O}(1)$ as \sqrt{s} increases and approaches M_X . This prediction is robust and can be tested by future e^+e^- colliders.

It is well-known that the oblique parameters[47] S and T constrain the mass splitting of the doublet scalars. In this model, H_5 and H_3 contribute

$$\Delta T_i = \frac{1}{16\pi s_W^2} \frac{M_{i+}^2}{M_W^2} \left[1 + z_i + \frac{2z_i}{1 - z_i} \ln z_i \right], \quad \Delta S_i = -\frac{1}{12\pi} \ln z_i, \quad (i = H_5, H_3), \quad (34)$$

where $z_i = (M_{i-}/M_{i+})^2$ is the ratio of $T_3 = -1/2$ charged component mass squared to that of the $T_3 = 1/2$ neutral component. Expanding around the degenerate case and denote $\Delta M_i = M_{i+} - M_{i-}$,

$$\Delta T_i \simeq \frac{1}{12\pi s_W^2} \frac{(\Delta M_i)^2}{M_W^2}, \quad \Delta S_i \simeq \frac{1}{6\pi} \frac{\Delta M_i}{M_{i+}}. \quad (35)$$

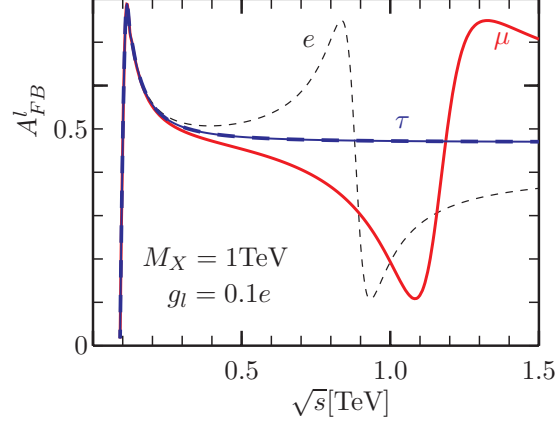


FIG. 8. Lepton forward-backward asymmetry for $M_X = 1\text{TeV}$, $g_l = 0.1e$, and $Q_l^N = -1$. If one adopts the other $U(1)_l$ charge assignment with the signs of all $U(1)_\ell$ charges flipped, then $A_{FB}^e \Leftrightarrow A_{FB}^\mu$.

ΔS_i can be either positive or negative, but ΔT_i is always positive. Thus, without any sign ambiguity, $\Delta T = \Delta T_5 + \Delta T_3$ can be used to constrain the model parameters. From $T_{exp} < 0.22$ at 95% C.L.[10],

$$\Delta M_5^2 + \Delta M_3^2 < 1.91 M_W^2. \quad (36)$$

Compared to $M_5, M_3 \sim \mathcal{O}(\text{TeV})$, both H_5 and H_3 have small mass splitting, $\lesssim M_W$. This implies that $\tilde{\lambda}_{H_3/H_5} \simeq \bar{\lambda}_{H_3/H_5}$ ⁸ and $|\kappa_{5,3}| < 1$ so that the mixings between $H_{5,3}$ and other scalars are small.

A. Effective Yukawa couplings

The loop-induced $h_{SM}\bar{e}e$ vertex yields an effective Yukawa coupling. Together with the tree-level contribution, the resulting effective electron-Higgs Yukawa coupling is the sum of two. We take the ratio to the SM electron-(125GeV Higgs) Yukawa, $y_{SM}^e = m_e/v_0$, and define the normalized electron-Higgs Yukawa as

$$\zeta_e = \frac{y_{eff}^{(e)}}{y_{SM}^e} = 1 + \bar{R}_e \times \left\{ -1 + A_0 + \left[s_2^2 - c_2 \left(\lambda_{H_3} + \tilde{\lambda}_{H_3} - \lambda_{H_6} \right) B_1 \right] A_1 + \left(\lambda_{H_3} + \tilde{\lambda}_{H_3} + \lambda_{H_6} \right) B_1 A_2 \right\}. \quad (37)$$

⁸ Another possibility is $|\tilde{\lambda}_{H_3}|, |\tilde{\lambda}_{H_5}|, |\bar{\lambda}_{H_3}|, |\bar{\lambda}_{H_5}| \ll 1$. Due the presence of $\kappa_{5,3}$ terms, one has to check numerically that the scalar potential is bounded from below.

In the above, the short-handed notations represent

$$\begin{aligned}
s_2 &= \sin(2\alpha^{(e)}), \quad c_2 = \cos(2\alpha^{(e)}), \quad B_1 = \frac{v_0^2}{M_N^2} \frac{1}{(z_H - z_L)}, \\
A_0 &= \frac{\mathcal{F}(z_L, z_H, z_h)}{\mathcal{F}_0(z_L, z_H)}, \\
A_1 &= \frac{\mathcal{F}(z_H, z_H, z_h) + \mathcal{F}(z_L, z_L, z_h) - 2\mathcal{F}(z_L, z_H, z_h)}{2\mathcal{F}_0(z_L, z_H)}, \\
A_2 &= \frac{\mathcal{F}(z_H, z_H, z_h) - \mathcal{F}(z_L, z_L, z_h)}{2\mathcal{F}_0(z_L, z_H)},
\end{aligned} \tag{38}$$

where $z_H = (M_H^{(e)}/M_N)^2$, $z_L = (M_L^{(e)}/M_N)^2$, $z_h = (q_h^2/M_N^2)$, and q_h is the 4-momentum carried by the SM Higgs. Numerically, the z_h contribution is insignificant, see Appendix B, $A_0 = 1 + \mathcal{O}(10^{-3})$, $A_1 > 0$, $A_2 < 0$, and the absolute values of $A_{1,2}$ increase as the ratio z_H/z_L gets bigger. We illustrate the normalized electron-Higgs Yukawa for one particular set of parameters in Fig.9. One can see that the electron-Higgs Yukawa can be very different, both in magnitude and sign, from the SM prediction. To better explore this model, we perform a numerical scan with $0.2\text{TeV} < M_L < M_H <$

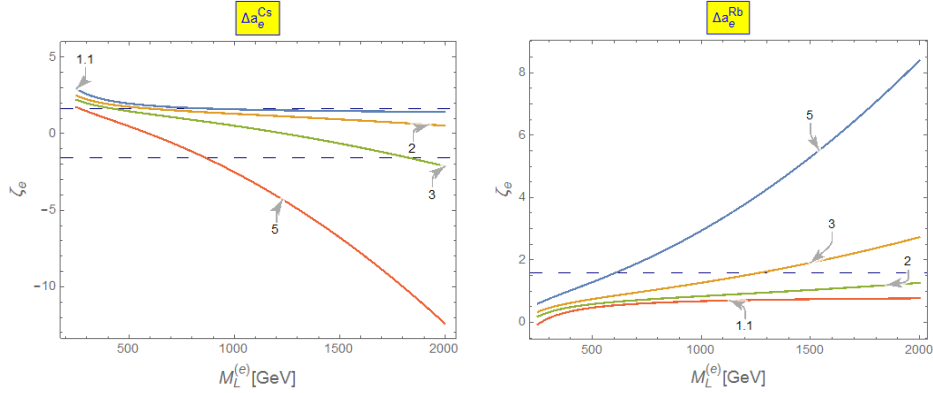


FIG. 9. The normalized electron-Higgs Yukawa ζ_μ vs $M_L^{(e)}$ for $M_H^{(e)}/M_L^{(e)} = \{1.1, 2, 3, 5\}$. Here we set $M_N = 1\text{TeV}$, $\sin(2\alpha^{(e)}) = 0.3$, $q_h^2 = (125\text{GeV})^2$, and $\lambda_{H3} = \tilde{\lambda}_{H3} = \lambda_{H6} = 1.0$. The horizontal dashed lines indicate the future experimental sensitivity, $|\zeta_e| < 1.6$ at FCC-ee[15].

10TeV , $\sin(2\alpha^{(e)}) \in [-.3, +.3]$, and each $\lambda_{H3}, \tilde{\lambda}_{H3}, \lambda_{H6} \in [0.1, \sqrt{4\pi}]$. The histogram of the resulting ζ_e is displayed in Fig.10, where the vertical dashed lines indicate the projected sensitivity, $|\zeta_e| < 1.6$ at 95% CL, at FCC-ee[15]. With the projected sensitivity at the FCC-ee, about 40.6(12.6)% of ζ_e for $\Delta a_e^{Cs(Rb)}$ can be detected. If adopting Δa_e^{Cs} , ζ_e spans from -33.1 to 5.4 and peaks in the range $[1.0, 2.0](\sim 70\%)$. The probability for $\{\zeta_e < -5, \zeta_e < -3, \zeta_e > 3\}$ are $\{2.3\%, 4.1\%, 0.45\%\}$, respectively. On the other hand, if Δa_e^{Rb} is adopted, ζ_e spans from -1.4 to 19.8 and peaks around $[0.5, 1.0](\sim 67\%)$. The chances for $\{\zeta_e > 5, \zeta_e > 3, \zeta_e < -1\}$ are $\{1.6\%, 4.7\%, 2 \times 10^{-4}\}$, respectively.

From the scan, we see that the abnormal electron-Higgs coupling is possible to be tested in the near future.

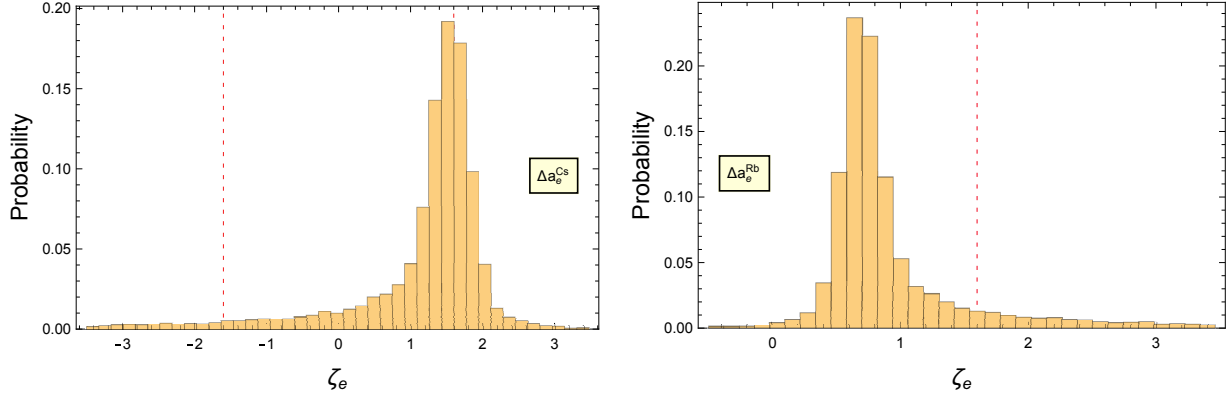


FIG. 10. The histogram of the normalized electron-Higgs Yukawa ζ_e . The vertical dashed lines indicate the future experimental sensitivity, $|\zeta_e| < 1.6$ at FCC-ee[15].

On the other hand, muon receives only the radiative mass correction such that $\overline{R}_\mu = 1$. In Fig.11, we display the normalized muon-Higgs Yukawa for a particular parameter set $\sin(2\alpha^{(\mu)}) = 0.1$ and $\lambda_{H5} = \tilde{\lambda}_{H5} = \lambda_{H8} = \lambda_\mu$. The effective muon-Higgs Yukawa is close to the SM one when $\lambda_\mu = 0.1$. If one adopts a larger coupling λ_μ , $\zeta_\mu < 1$, it could be as small as ~ 0.4 when $\lambda_\mu = 3$ and $M_N = 2\text{TeV}$. It usually stays within the current 2σ constraint, $0.6 \lesssim \zeta_\mu \lesssim 1.5$ [6, 7]. We also

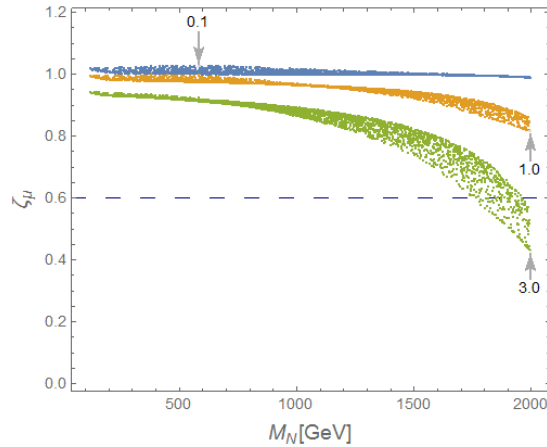


FIG. 11. The normalized muon-Higgs Yukawa ζ_μ vs M_N . Here we set $\Delta a_\mu = 25.1 \times 10^{-10}$, $\sin(2\alpha^{(\mu)}) = 0.1$, and $\lambda_{H5} = \tilde{\lambda}_{H5} = \lambda_{H8} = \{0.1, 1.0, 3.0\}$. The horizontal dashed line is the current experimental lower limit on $\zeta_\mu > 0.6$ [6, 7].

perform a numerical scan over the ranges: $M_N \in [0.2, 2.0]\text{TeV}$, $\sin(2\alpha^\mu) \in [-0.3, 0.3]$, and each $\lambda_{H5}, \tilde{\lambda}_{H5}, \lambda_{H8} \in [0.1, \sqrt{4\pi}]$. The histogram of the resulting ζ_μ is shown in Fig.12. The normalized

muon Yukawa spans from 0.38 to 1.21 and mostly peaks in the range of $[0.8, 1.0]$ ($\sim 82.0\%$), with the chance of $\sim 7.5\%$ (0.66%), for ζ_μ being greater than 1.0 (or smaller than the current lower bound 0.6). See [11] for the future updates of ζ_μ at HL-LHC and e^+e^- colliders. With the ultima

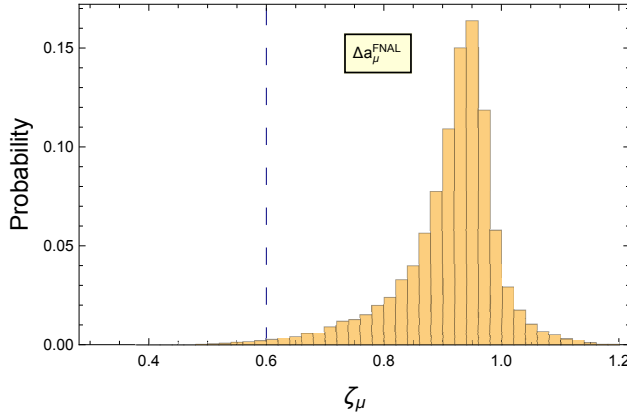


FIG. 12. The histogram of the normalized muon-Higgs Yukawa ζ_μ . The vertical dashed line indicates the current experimental lower limit on $\zeta_\mu > 0.6$ [6, 7].

projected precision of $\sim 0.4\%$ at the future FCC[12], the entire range of predicted muon-Yukawa can be covered and probed.

V. DARK MATTER AND NEUTRINO MASSES

The current model does not have a dark matter (DM) candidate. However, with the gauged $U(1)_\ell$ symmetry, DM candidate can be easily included by extending the particle content. One can introduce a pair of vector fermion D which only interacts with the gauge boson X by adjusting its $U(1)_\ell$ charge, Q_D ⁹. Then D can be assigned with a dark parity without upsetting any gauge symmetry. This dark parity remains even after the SSB of $U(1)_\ell$ and SM electroweak, making D a DM candidate. The annihilation cross section of $D\bar{D} \rightarrow X^* \rightarrow f\bar{f}$ can be calculated to be

$$\langle\sigma v\rangle_{D\bar{D}\rightarrow f\bar{f}} \simeq Q_D^2 g_l^4 \frac{(G_L^f)^2 + (G_R^f)^2}{\sqrt{2}\pi M_X^2} \frac{\beta_D}{(1-4\beta_D)^2}, \quad (39)$$

where $\beta_D = (M_D/M_X)^2$. Since the third generation lepton is $U(1)_l$ neutral, the final states can be l^+l^- or $\bar{\nu}_l\nu_l$ and $l = e, \mu$. From $\Omega_{DM}h^2 = 0.120 \pm 0.001$ [48] and $\Omega_{DM}h^2 \simeq 4.8 \times 10^{-10}(\text{GeV})^{-2}/\langle\sigma v\rangle$, we obtain

$$\left(\frac{Q_D}{10}\right)^2 \left(\frac{g_l}{e}\right)^4 \frac{1}{M_X^2} \frac{\beta_D}{(1-4\beta_D)^2} \simeq 1.1 \times 10^{-10}(\text{GeV})^{-2}. \quad (40)$$

⁹ There are infinite possible Q_D 's that forbid all Yukawa couplings between D and other fields. $Q_D = 10$ and $Q_D = 1/2$ are two concrete examples.

For $M_X = 1\text{TeV}$, $Q_D = 10$, and $g_l = 0.1e$, either $M_D = 0.394\text{TeV}$ or $M_D = 0.633\text{TeV}$ can yield the correct DM relic density. Moreover, since D is leptophilic, it can safely escape the direct search bound.

Finally, we comment on how to generate the active neutrino masses in this model. The Majorana neutrino mass matrix element \mathcal{M}_{ij}^ν can arise from the corresponding Weinberg operator[49] $(L_i H)(L_j H)$. However, the traditional lepton number is conserved in the current model, which forbids the Weinberg operator. One possible simple extension is introducing an extra $U(1)_\ell$ charge-2 scalar S_2 and allowing it to develop VEV¹⁰. Therefore, the $U(1)_l$ charge of every Weinberg operator can be balanced, and the observed neutrino oscillation data can be explained at the price of potential CLFV. In that case, one must carefully consider the stringent CLFV constraints (see [43], for example), and the comprehensive analysis is beyond the scope of this paper.

VI. CONCLUSION

We have proposed an anomaly-free gauged lepton number $U(1)_\ell$ symmetry where the observed $\Delta a_{e,\mu}$ are explained, and the charged lepton mass hierarchy arises naturally. On top of the SM particle content, this model requires one pair of vector fermions, two scalar doublets, and three scalar singlets, see Table II, with TeV-ish masses. The flavor-dependent $U(1)_\ell$ charge assignment, see Table I, is novel to our best knowledge. In our model, tau picks up its mass via the SM Yukawa interaction, while the $U(1)_\ell$ charge assignment forbids the SM Yukawa interactions for electron and muon. Both electron and muon acquire a radiatively generated mass from the photon-removed one-loop diagrams for the observed $\Delta a_{e,\mu}$. Electron receives an extra mass contribution from its coupling to SM Higgs mediated by one of the exotic doublet scalars. Compared to the SM tau Yukawa coupling, this model does not require extreme model parameters to reproduce the observed $m_{e,\mu}$ and $\Delta a_{e,\mu}$.

This model has two nice features: (1) either positive $\Delta a_e^{Rb} \simeq 4.8 \times 10^{-13}$ [37] or negative $\Delta a_e^{Cs} \simeq -8.7 \times 10^{-13}$ [36] can be accommodated with $\Delta a_\mu^{BNL-FNAL} \simeq 25.1 \times 10^{-10}$ [30] in this model, and (2) without any ad hoc symmetries or parities introduced, the automatically emerged conventional lepton number and tau-parity ensure that the tau flavor is conserved to all orders in this model. We have also proved that in the $e - \mu$ sector, all the dim-4 and dim-6 CLFV SM operators vanish to all orders. Hence, no CLFV constraint on this model is expected in the foreseeable future.

¹⁰ This also allows the vector fermion N to acquire a Majorana mass and breaks the traditional lepton number, see[43].

We have discussed the phenomenology and pointed out two testable signatures of this model: (1) depending on the overall sign of $U(1)_\ell$ charges, we predicted either $A_{FB}^e > A_{FB}^\tau > A_{FB}^\mu$ or $A_{FB}^e < A_{FB}^\tau < A_{FB}^\mu$. This can be tested at the future e^+e^- colliders before the direct discovery of the $U(1)_\ell$ gauge boson. (2) The abnormal electron- and muon-Higgs Yukawa couplings. Our numerical study found that $-33 \lesssim y_{eff}^{(e)}/y_{SM}^e \lesssim 20$ and $0.6 \lesssim y_{eff}^{(\mu)}/y_{SM}^\mu \lesssim 1.2$, which could be probed in the HL-LHC or future e^+e^- colliders.

Finally, this simple model with this specific $U(1)_\ell$ charge assignment can be ruled out if: (1) any tau flavor violation is confirmed or (2) $|\Delta a_\tau| > 10^{-10}$ is observed.

ACKNOWLEDGMENTS

This research is supported by MOST 109-2112-M-007-012 and 110-2112-M-007-028 of Taiwan.

Appendix A: Scalar sector

Here we spell out the most general scalar sector lagrangian for this model. The relevant lagrangian can be written as

$$\mathcal{L} \supset \mathcal{L}_1 - V_1 - V_2. \quad (\text{A1})$$

The kinetic and quadratic terms are collected in \mathcal{L}_1 :

$$\begin{aligned} \mathcal{L}_1 = & (D_\mu H)^\dagger (D^\mu H) + (D_\mu H_5)^\dagger (D^\mu H_5) + (D_\mu H_3)^\dagger (D^\mu H_3) \\ & + (D_\mu C_6)^\dagger (D^\mu C_6) + (D_\mu C_8)^\dagger (D^\mu C_8) + (D_\mu S_3)^\dagger (D^\mu S_3) \\ & + \mu^2 H^\dagger H - M_5^2 H_5^\dagger H_5 - M_3^2 H_3^\dagger H_3 - M_6^2 |C_6|^2 - M_8^2 |C_8|^2 + \mu_l^2 |S_3|^2, \end{aligned} \quad (\text{A2})$$

where the covariant derivative is

$$D_\mu = \partial_\mu - ig_2 |T_3| \vec{\sigma} \cdot \vec{A}_\mu - ig_1 Y B_\mu - ig_l Q_l X_\mu. \quad (\text{A3})$$

The gauge invariant renormalizable quartic coupling potential is

$$\begin{aligned} V_1 = & \lambda_H (H^\dagger H)^2 + \lambda_{H5} (H^\dagger H) (H_5^\dagger H_5) + \lambda_{H3} (H^\dagger H) (H_3^\dagger H_3) + \lambda_{H6} (H^\dagger H) |C_6|^2 + \lambda_{H8} (H^\dagger H) |C_8|^2 \\ & + \lambda_{Hl} (H^\dagger H) |S_3|^2 + \lambda_5 (H_5^\dagger H_5)^2 + \lambda_{53} (H_5^\dagger H_5) (H_3^\dagger H_3) + \lambda_{56} (H_5^\dagger H_5) |C_6|^2 + \lambda_{58} (H_5^\dagger H_5) |C_8|^2 \\ & + \lambda_{5l} (H_5^\dagger H_5) |S_3|^2 + \lambda_3 (H_3^\dagger H_3)^2 + \lambda_{36} (H_3^\dagger H_3) |C_6|^2 + \lambda_{38} (H_3^\dagger H_3) |C_8|^2 + \lambda_{3l} (H_3^\dagger H_3) |S_3|^2 \\ & + \lambda_6 |C_6|^4 + \lambda_{68} |C_6|^2 |C_8|^2 + \lambda_{6l} |C_6|^2 |S_3|^2 + \lambda_8 |C_8|^4 + \lambda_{8l} |C_8|^2 |S_3|^2 + \lambda_l |S_3|^4 \\ & + \tilde{\lambda}_{H5} (H^\dagger H_5) (H_5^\dagger H) + \tilde{\lambda}_{H3} (H^\dagger H_3) (H_3^\dagger H) + \tilde{\lambda}_{53} (H_5^\dagger H_3) (H_3^\dagger H_5) \\ & + \bar{\lambda}_{H5} (H^\dagger \tilde{H}_5) (\tilde{H}_5^\dagger H) + \bar{\lambda}_{H3} (H^\dagger \tilde{H}_3) (\tilde{H}_3^\dagger H) + \bar{\lambda}_{53} (H_5^\dagger \tilde{H}_3) (\tilde{H}_3^\dagger H_5). \end{aligned} \quad (\text{A4})$$

Also, we have

$$V_2 = \mu_{H_3} H^\dagger \tilde{H}_3 S_3^* + \kappa_3 H^\dagger H_3 S_3^* C_6 + \kappa_5 H^\dagger H_5 S_3 C_8 + H.c. \quad (\text{A5})$$

From the above, the mass matrix for the charged scalars after SSB can be read

$$\mathcal{L} \supset -(H_3^+, C_6^+) \mathcal{M}_{36} \begin{pmatrix} H_3^- \\ C_6^- \end{pmatrix} - (H_5^+, C_8^+) \mathcal{M}_{58} \begin{pmatrix} H_5^- \\ C_8^- \end{pmatrix}, \quad (\text{A6})$$

where

$$\mathcal{M}_{36} = \begin{pmatrix} M_3^2 + \frac{\lambda_{H_3} + \tilde{\lambda}_{H_3}}{2} v_0^2 + \frac{\lambda_{3L}}{2} v_3^2 & \frac{1}{2} \kappa_3 v_0 v_3 \\ \frac{1}{2} \kappa_3 v_0 v_3 & M_6^2 + \frac{\lambda_{H_6}}{2} v_0^2 + \frac{\lambda_{6L}}{2} v_3^2 \end{pmatrix}, \quad (\text{A7})$$

and a similar form for \mathcal{M}_{58} . Also, the couplings between the charged scalars and the neutral component of the SM Higgs doublet h is

$$\mathcal{L} \supset -h(H_3^+, C_6^+) \Lambda_{36} \begin{pmatrix} H_3^- \\ C_6^- \end{pmatrix}, \quad \Lambda_{36} = \begin{pmatrix} (\lambda_{H_3} + \tilde{\lambda}_{H_3}) v_0 & \frac{1}{2} \kappa_3 v_3 \\ \frac{1}{2} \kappa_3 v_3 & \lambda_{H_6} v_0 \end{pmatrix}. \quad (\text{A8})$$

Appendix B: 1-loop function

When evaluating the Feynman diagrams displayed in Fig.1, one encounters the following integral

$$\mathcal{F}(a, b, c) = \int_0^1 dx \int_0^{1-x} dy \frac{1}{1-x-y+ax+by-xy}, \quad (\text{B1})$$

where $a, b, c \geq 0$. As long as $c < 4\sqrt{ab}$, $\mathcal{F}(a, b, c)$ is always positive. For $c \ll a, b$, the loop integral can be expanded as

$$\mathcal{F}(a, b, c) = \mathcal{F}_0(a, b) + c \mathcal{F}_1(a, b) + \mathcal{O}(c^2), \quad (\text{B2})$$

where

$$\begin{aligned} \mathcal{F}_0(a, b) &= \frac{1}{a-b} \left(\frac{a \ln a}{a-1} - \frac{b \ln b}{b-1} \right), \\ \mathcal{F}_1(a, b) &= \int_0^1 dx \int_0^{1-x} dy \frac{xy}{(1-x-y+ax+by)^2}. \end{aligned} \quad (\text{B3})$$

For the parameter space we are interested in, $0.2 \text{ TeV} < M_N < 2 \text{ TeV}$ and $0.5 \text{ TeV} < M_{L_i} < M_{H_i} < 10 \text{ TeV}$, $10^{-5} < \mathcal{F}_1/\mathcal{F}_0 < 0.5$. Moreover,

$$\mathcal{F}_0(a, b) \rightarrow \frac{a-1-\ln a}{(a-1)^2}, \quad \text{when } a \rightarrow b. \quad (\text{B4})$$

Appendix C: Forward-backward asymmetry

The tree level forward-backward asymmetry of $e^+e^- \rightarrow f\bar{f}$ due to the interference among photon, Z , and X can be easily calculated and summarized as

$$\begin{aligned} A_{FB}^f(s) &\equiv \frac{\sigma^F(e^+e^- \rightarrow f\bar{f}) - \sigma^B(e^+e^- \rightarrow f\bar{f})}{\sigma^F(e^+e^- \rightarrow f\bar{f}) + \sigma^B(e^+e^- \rightarrow f\bar{f})} \\ &= \frac{3 \sum_{a,b=\gamma,Z,X} K_{ab}(s)(L_{ab}^e - R_{ab}^e)(L_{ab}^f - R_{ab}^f)}{4 \sum_{a,b=\gamma,Z,X} K_{ab}(s)(L_{ab}^e + R_{ab}^e)(L_{ab}^f + R_{ab}^f)}. \end{aligned} \quad (\text{C1})$$

The interfering terms are given by

$$K_{ab}(s) = (2 - \delta_{ab}) \Re \left[\left(1 - \frac{M_a^2}{s} + i \frac{M_a \Gamma_a}{s} \right)^{-1} \left(1 - \frac{M_b^2}{s} - i \frac{M_b \Gamma_b}{s} \right)^{-1} \right], \quad (\text{C2})$$

where s is the CM energy squared, and the Kronecker delta function takes care of the proper factors. The short handed notations are defined as

$$L_{ab}^f = G_{aL}^f G_{bL}^f, \quad R_{ab}^f = G_{aR}^f G_{bR}^f, \quad (\text{C3})$$

where $G_{L/R}$ is the gauge couplings normalized to e . Namely, $G_{\gamma,L/R}^f = Q^f$, $G_{Z,L/R}^f = (T_3 - Q)_{L/R}^f / (c_W s_W)$, and $G_{X,L/R}^f = (g_l/e) Q_{L/R}^f$.

-
- [1] M. Aaboud *et al.* (ATLAS), Measurements of Higgs boson properties in the diphoton decay channel with 36 fb^{-1} of pp collision data at $\sqrt{s} = 13 \text{ TeV}$ with the ATLAS detector, *Phys. Rev. D* **98**, 052005 (2018), arXiv:1802.04146 [hep-ex].
 - [2] M. Aaboud *et al.* (ATLAS), Observation of $H \rightarrow b\bar{b}$ decays and VH production with the ATLAS detector, *Phys. Lett. B* **786**, 59 (2018), arXiv:1808.08238 [hep-ex].
 - [3] A. M. Sirunyan *et al.* (CMS), Observation of Higgs boson decay to bottom quarks, *Phys. Rev. Lett.* **121**, 121801 (2018), arXiv:1808.08242 [hep-ex].
 - [4] G. Aad *et al.* (ATLAS), Evidence for the Higgs-boson Yukawa coupling to tau leptons with the ATLAS detector, *JHEP* **04**, 117, arXiv:1501.04943 [hep-ex].
 - [5] A. M. Sirunyan *et al.* (CMS), Observation of the Higgs boson decay to a pair of τ leptons with the CMS detector, *Phys. Lett. B* **779**, 283 (2018), arXiv:1708.00373 [hep-ex].
 - [6] G. Aad *et al.* (ATLAS), A search for the dimuon decay of the Standard Model Higgs boson with the ATLAS detector, *Phys. Lett. B* **812**, 135980 (2021), arXiv:2007.07830 [hep-ex].
 - [7] A. M. Sirunyan *et al.* (CMS), Evidence for Higgs boson decay to a pair of muons, *JHEP* **01**, 148, arXiv:2009.04363 [hep-ex].

- [8] G. Aad *et al.* (ATLAS), Combined measurements of Higgs boson production and decay using up to 80 fb^{-1} of proton-proton collision data at $\sqrt{s} = 13 \text{ TeV}$ collected with the ATLAS experiment, *Phys. Rev. D* **101**, 012002 (2020), arXiv:1909.02845 [hep-ex].
- [9] A. M. Sirunyan *et al.* (CMS), Combined measurements of Higgs boson couplings in proton-proton collisions at $\sqrt{s} = 13 \text{ TeV}$, *Eur. Phys. J. C* **79**, 421 (2019), arXiv:1809.10733 [hep-ex].
- [10] P. A. Zyla *et al.* (Particle Data Group), Review of Particle Physics, *PTEP* **2020**, 083C01 (2020).
- [11] J. de Blas *et al.*, Higgs Boson Studies at Future Particle Colliders, *JHEP* **01**, 139, arXiv:1905.03764 [hep-ph].
- [12] A. Abada *et al.* (FCC), FCC Physics Opportunities: Future Circular Collider Conceptual Design Report Volume 1, *Eur. Phys. J. C* **79**, 474 (2019).
- [13] V. Khachatryan *et al.* (CMS), Search for a standard model-like Higgs boson in the $\mu^+\mu^-$ and e^+e^- decay channels at the LHC, *Phys. Lett. B* **744**, 184 (2015), arXiv:1410.6679 [hep-ex].
- [14] G. Aad *et al.* (ATLAS), Search for the Higgs boson decays $H \rightarrow ee$ and $H \rightarrow e\mu$ in pp collisions at $\sqrt{s} = 13 \text{ TeV}$ with the ATLAS detector, *Phys. Lett. B* **801**, 135148 (2020), arXiv:1909.10235 [hep-ex].
- [15] D. d’Enterria, A. Poldaru, and G. Wojcik, Measuring the electron Yukawa coupling via resonant s-channel Higgs production at FCC-ee, *Eur. Phys. J. Plus* **137**, 201 (2022), arXiv:2107.02686 [hep-ex].
- [16] K. S. Babu and E. Ma, Radiative Mechanisms for Generating Quark and Lepton Masses: Some Recent Developments, *Mod. Phys. Lett. A* **4**, 1975 (1989).
- [17] B. A. Dobrescu and P. J. Fox, Quark and lepton masses from top loops, *JHEP* **08**, 100, arXiv:0805.0822 [hep-ph].
- [18] H. Okada and K. Yagyu, Radiative generation of lepton masses, *Phys. Rev. D* **89**, 053008 (2014), arXiv:1311.4360 [hep-ph].
- [19] E. Ma, Radiative Origin of All Quark and Lepton Masses through Dark Matter with Flavor Symmetry, *Phys. Rev. Lett.* **112**, 091801 (2014), arXiv:1311.3213 [hep-ph].
- [20] E. Gabrielli, L. Marzola, and M. Raidal, Radiative Yukawa Couplings in the Simplest Left-Right Symmetric Model, *Phys. Rev. D* **95**, 035005 (2017), arXiv:1611.00009 [hep-ph].
- [21] S. Weinberg, Models of Lepton and Quark Masses, *Phys. Rev. D* **101**, 035020 (2020), arXiv:2001.06582 [hep-th].
- [22] E. Ma, Split Left-Right Symmetry and Scotogenic Quark and Lepton Masses, *Phys. Lett. B* **811**, 135971 (2020), arXiv:2010.09127 [hep-ph].
- [23] M. J. Baker, P. Cox, and R. R. Volkas, Radiative muon mass models and $(g - 2)_\mu$, *JHEP* **05**, 174, arXiv:2103.13401 [hep-ph].
- [24] C.-W. Chiang and K. Yagyu, Radiative Seesaw Mechanism for Charged Leptons, *Phys. Rev. D* **103**, L111302 (2021), arXiv:2104.00890 [hep-ph].
- [25] W. Yin, Radiative lepton mass and muon $g - 2$ with suppressed lepton flavor and CP violations, *JHEP* **08**, 043, arXiv:2103.14234 [hep-ph].

- [26] A. E. C. Hernández, S. Kovalenko, M. Maniatis, and I. Schmidt, Fermion mass hierarchy and $g - 2$ anomalies in an extended 3HDM Model, *JHEP* **10**, 036, arXiv:2104.07047 [hep-ph].
- [27] R. Adhikari, I. A. Bhat, D. Borah, E. Ma, and D. Nanda, Anomalous magnetic moment and Higgs coupling of the muon in a sequential $U(1)$ gauge model with dark matter, *Phys. Rev. D* **105**, 035006 (2022), arXiv:2109.05417 [hep-ph].
- [28] S. Jana, S. Klett, and M. Lindner, Flavor seesaw mechanism, *Phys. Rev. D* **105**, 115015 (2022), arXiv:2112.09155 [hep-ph].
- [29] G. Mohanta and K. M. Patel, Radiatively generated fermion mass hierarchy from flavour non-universal gauge symmetries, (2022), arXiv:2207.10407 [hep-ph].
- [30] B. Abi *et al.* (Muon $g-2$), Measurement of the Positive Muon Anomalous Magnetic Moment to 0.46 ppm, *Phys. Rev. Lett.* **126**, 141801 (2021), arXiv:2104.03281 [hep-ex].
- [31] T. Aoyama *et al.*, The anomalous magnetic moment of the muon in the Standard Model, *Phys. Rept.* **887**, 1 (2020), arXiv:2006.04822 [hep-ph].
- [32] S. Borsanyi *et al.*, Leading hadronic contribution to the muon magnetic moment from lattice QCD, *Nature* **593**, 51 (2021), arXiv:2002.12347 [hep-lat].
- [33] M. Cè *et al.*, Window observable for the hadronic vacuum polarization contribution to the muon $g-2$ from lattice QCD, *Phys. Rev. D* **106**, 114502 (2022), arXiv:2206.06582 [hep-lat].
- [34] C. Alexandrou *et al.*, Lattice calculation of the short and intermediate time-distance hadronic vacuum polarization contributions to the muon magnetic moment using twisted-mass fermions, (2022), arXiv:2206.15084 [hep-lat].
- [35] C. T. H. Davies *et al.* (Fermilab Lattice, MILC, HPQCD), Windows on the hadronic vacuum polarization contribution to the muon anomalous magnetic moment, *Phys. Rev. D* **106**, 074509 (2022), arXiv:2207.04765 [hep-lat].
- [36] R. H. Parker, C. Yu, W. Zhong, B. Estey, and H. Müller, Measurement of the fine-structure constant as a test of the Standard Model, *Science* **360**, 191 (2018), arXiv:1812.04130 [physics.atom-ph].
- [37] L. Morel, Z. Yao, P. Cladé, and S. Guellati-Khélifa, Determination of the fine-structure constant with an accuracy of 81 parts per trillion, *Nature* **588**, 61 (2020).
- [38] W. Chao, Pure Leptonic Gauge Symmetry, Neutrino Masses and Dark Matter, *Phys. Lett. B* **695**, 157 (2011), arXiv:1005.1024 [hep-ph].
- [39] P. Schwaller, T. M. P. Tait, and R. Vega-Morales, Dark Matter and Vectorlike Leptons from Gauged Lepton Number, *Phys. Rev. D* **88**, 035001 (2013), arXiv:1305.1108 [hep-ph].
- [40] W.-F. Chang and J. N. Ng, Study of Gauged Lepton Symmetry Signatures at Colliders, *Phys. Rev. D* **98**, 035015 (2018), arXiv:1805.10382 [hep-ph].
- [41] W.-F. Chang and J. N. Ng, Neutrino masses and gauged $U(1)_\ell$ lepton number, *JHEP* **10**, 015, arXiv:1807.09439 [hep-ph].
- [42] W.-F. Chang and J. N. Ng, Alternative Perspective on Gauged Lepton Number and Implications for Collider Physics, *Phys. Rev. D* **99**, 075025 (2019), arXiv:1808.08188 [hep-ph].

- [43] W.-F. Chang and S.-H. Kuo, Possibly heteroclitic electron Yukawa coupling and small Δa_μ in a hidden Abelian gauge model for neutrino masses, (2022), arXiv:2206.14394 [hep-ph].
- [44] W.-F. Chang, One colorful resolution to the neutrino mass generation, three lepton flavor universality anomalies, and the Cabibbo angle anomaly, (2021), arXiv:2105.06917 [hep-ph].
- [45] V. Andreev *et al.* (ACME), Improved limit on the electric dipole moment of the electron, *Nature* **562**, 355 (2018).
- [46] G. W. Bennett *et al.* (Muon (g-2)), An Improved Limit on the Muon Electric Dipole Moment, *Phys. Rev. D* **80**, 052008 (2009), arXiv:0811.1207 [hep-ex].
- [47] M. E. Peskin and T. Takeuchi, A New constraint on a strongly interacting Higgs sector, *Phys. Rev. Lett.* **65**, 964 (1990).
- [48] N. Aghanim *et al.* (Planck), Planck 2018 results. VI. Cosmological parameters, *Astron. Astrophys.* **641**, A6 (2020), [Erratum: *Astron. Astrophys.* 652, C4 (2021)], arXiv:1807.06209 [astro-ph.CO].
- [49] S. Weinberg, Baryon and Lepton Nonconserving Processes, *Phys. Rev. Lett.* **43**, 1566 (1979).